X-radiographic Images of Shock Waves Generated by High-pressure Diesel Sprays

A. MacPhee,[1] C. F. Powell,[1] Y. Yue,[1] S. Narayanan,[1] J. Wang,[1] M. W. Tate,[2]
M. J. Renzi,[2] A. Ercan,[2] E. Fontes,[2] S. M. Gruner,[2] J. Walther,[3] J. Schaller[3]

[1]Argonne National Laboratory, Argonne, IL, U.S.A.
[2]Cornell University, Ithaca, NY, U.S.A.
[3]Corporate Research, Robert Bosch GmbH, Stuttgart, Germany

Introduction

High-pressure, high-speed sprays are essential for many industrial and consumer applications, including fuel injection systems, inkjet printers, liquid-jet cutting tools, and liquid-jet cleaning systems [1, 2]. Often the liquids are optically dense, or the liquid droplets generated by the sprays scatter light so strongly that the detailed structure of the sprays cannot be resolved by conventional optical means. Such conditions are found to be true especially in the region near the injection nozzle, and this is often the region of greatest interest with regard to understanding the structure of the jet. Other challenges arise from the transient nature of the features of jet sprays; frequently, images are required on microsecond timescales. The lack of quantitative, time-resolved analyses of the structure and dynamics of sprays limits the accuracy of spray modeling and creates obstacles to improving spray technology. Improvements of even a few percent would have enormously important and beneficial economic and social consequences. This knowledge has spurred considerable activity in the development of optical techniques for measuring diesel fuel injection systems. Despite significant advances in diagnostics over the last 20 years, the region close to the nozzle has not satisfactorily yielded to experiments designed to acquire quantitative information [2-8]. Multiple scattering from the large number of droplets prevents the penetration of light in this near-nozzle region, thus limiting quantitative evaluation with these techniques. In this research, we report not only that the dense part of the fuel spray has been effectively and quantitatively probed by a nonintrusive method using monochromatic x-radiographic techniques but also that complicated hydrodynamic phenomena, such as shock waves generated by high-speed diesel sprays, have been quantitatively detected and visualized in a direct manner [9-11].

Methods and Materials

The experimental setup uses fuel injection into a chamber with x-ray-transparent windows. To study diesel fuel injection, we employed a high-pressure common rail injection system typical of that in a passenger car but with a specially fabricated single-orifice nozzle. The nozzle was 180 μm in diameter, and the injection pressure could be set between 500 and 1350 bar. Fuel was injected into a spray chamber filled with inert gas (SF_6) at atmospheric pressure and room temperature (typically 25-30°C). SF_6, which is a heavy gas (molecular weight of 146), was used to simulate the relatively dense ambient gas environment in a diesel engine during the adiabatic compression part of the engine cycle when the diesel fuel is normally injected. The fuel used in this study was a blend of No. 2 diesel (Amoco) and a cerium-containing compound (DPX9, Rhodia Terres Rares, 4.2 wt% in the blend). The time-resolved radiograph experiments on the diesel fuel sprays were performed in two steps: (1) by scanning with a small x-ray beam and a point detector [9, 10] and (2) by using a beam of extended size with a fast area detector [11]. In the first step, the radiographic images of the sprays were collected by a focused and monochromatic synchrotron x-ray beam from bending magnet beamline 1-BM at the APS in conjunction with a fast avalanche photodiode (APD) point detector [9]. The second step of the experiment involved imaging the spray process and propagating the shock waves with a pixel array detector (PAD) [12, 13] with a spatially extended, wide-bandpass synchrotron x-ray beam at the D-1 beamline of the Cornell High Energy Synchrotron Source (CHESS) [11].

Optical Schlieren images [14] of the shock waves generated by fuel sprays in SF_6 gas were collected before the x-ray measurements were made under similar injection conditions. To visualize the density change in the shock front in the gas medium, flashing white light was collimated by an aperture and a collimating lens before illuminating the fuel sprays. The images were collected at the Schlieren plane. The exposure time was controlled by a gated image intensifier to a duration of about 0.1 μs.

Results

On the basis of the point absorption measurements, the time-resolved fuel-mass data measured on the central spray axis at distances of 1, 5, 12, and 22 mm from the nozzle are shown in Fig. 1a. These plots show features typically found on the spray axis. For the data collected at
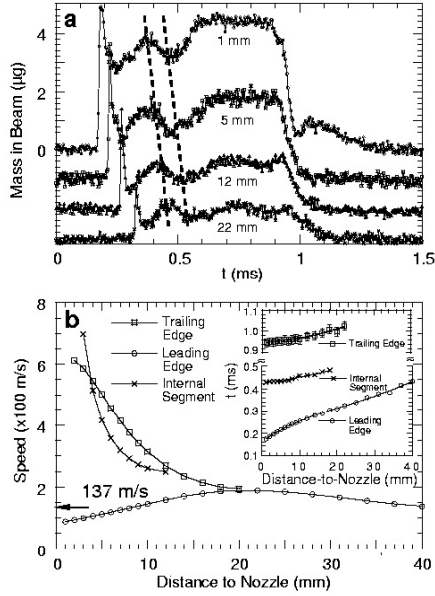
FIG. 1. Dynamics of the high-pressure fuel sprays: (a) the time evolution of the integrated fuel mass on the spray axis at 1, 5, 12, and 22 mm from the nozzle and (b) the calculated spray speed. The speed of a spray segment between the two broken lines in (a) was evaluated by using the correlation method illustrated in Ref. 11.

1 mm, the spray intersected the x-ray at t = 0.166 ms, evidenced by an abrupt increase in the fuel mass from 0 to nearly 5 μg. This leading edge of the fuel spray appears abruptly, indicating a distinct boundary between ambient gas and fuel spray. The sharpness of the interface facilitates the calculation of the apparent speed of the leading edge of the spray, as shown in Fig. 1b. Immediately after the leading edge is a highly concentrated fuel region represented by an extremely sharp peak that shows a change width in time from about 20 μs at 1 mm to less than 10 μs at 12 mm. While the injection pressure remained more stable during the injection (data not shown), the fuel mass in the spray body appeared to be fluctuating with rather large amplitudes. Although not as sharp as the leading edge, the spray trailing edge is well defined and appeared at close to the 1-ms mark, indicating that the injection event had finished.

The trailing edge of the jet is interesting in that it clearly illustrates the dynamics of the injection process, since the trailing edge moves at an instantaneous speed much greater than that of the leading edge, at least in the region close to the nozzle (see data collected at 1 and 5 mm in Fig. 1a). Indeed, the calculation of the position dependence of the speed, shown in Fig. 1b, proved the direct observation. As the spray exited the nozzle, the

leading edge appeared to accelerate from 90 to about 180 m/s. It is quite striking that the trailing edge speed was greater than 600 m/s, well above the sonic speed of SF_6 of 137 m/s [15], when the spray had just exited the nozzle. Thereafter, the trailing edge slowed down to 180 m/s at 20 mm from the nozzle, where it was equal to the leading edge speed; after this, the leading edge speed started to decrease, as expected. Because the spray was composed of an aerosol of streams and droplets, the liquid at the leading edge of the spray could move at rates quite different than those of the average body of the spray.

To further prove this point, one can take advantage of the density fluctuations shown in the time-resolved mass profiles (Fig. 1a). The fluctuations indicate that the axial mass distribution is not uniform throughout the spray body. The first sharp peak in the mass profile is almost certainly caused by mass accumulation as the droplets affect the chamber gas. We speculate that the fluctuations are the result of gas entrainment near the nozzle exit. Fortunately, these fluctuations allowed us to perform a correlation calculation for evaluating the internal speed of the spray body, as in Ref. 11. The speeds that are calculated in this way (Fig. 1b) lie between the speeds for the leading and trailing edges but are much closer to the speed for the trailing edge. Therefore, we conclude that the major part of the spray travels in the injection chamber at a speed much higher than the speed of sound in the SF_6 gas. In addition, we should point out that the calculation also shows that a small part of the spray has a speed rather similar to that of the leading edge and travels below the speed of sound. Although the point detector measurements described so far suggest that the fuel spray should generate shock waves, the point-by-point method lacked the spatial resolution and coverage to directly image the shock waves.

Recently, the shock waves were visualized in the same spray system by Schlieren imaging of visible light (images not shown). The shock-wave front can be clearly observed when the injection pressure reaches 800 bar, the pressure at which the images in Fig. 2 were taken. The figure also shows that the shock front can be reflected to the spray. The shock-wave effect on atomization and the possibility of facilitating better atomization of the liquid fuel near the nozzle by the shock waves are being investigated.

Direct imaging of the shock waves became possible with the development of the PAD [12, 13]. Figure 2 shows a series of x-radiographs of the fuel spray for times ranging from 38 to 192 μs after the beginning of the injection process. The false-color levels of the images have been set to accentuate small differences in the x-ray intensity arising from the slightly increased x-ray absorption in the compressed SF_6 gas. The shock-wave front, or so-called Mach cone, is clearly seen as emanating from the leading edge of the fuel jet. The Mach cone angles were also measured at each instance, and the values
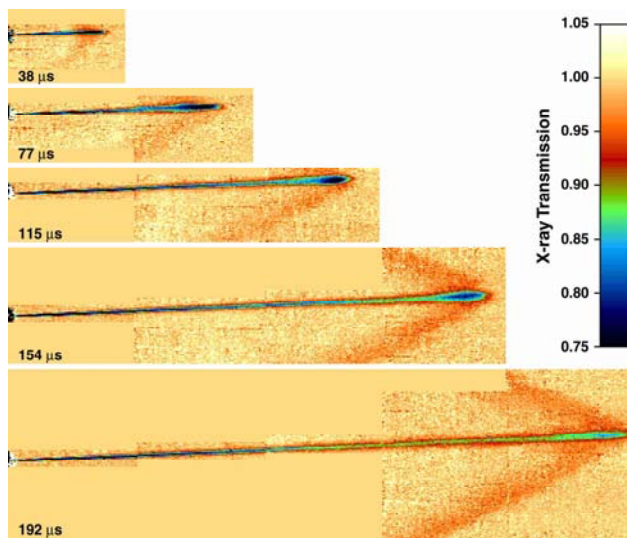
FIG. 2. Time-resolved radiographic images of fuel sprays and the shock waves generated by the sprays for time instances of 38, 77, 115, 154, and 192 µs after the start of the injection. A total of 168 frames were taken.

agreed well with the leading edge speed determined by the analysis outlined in Fig. 1.

The quantitative nature of the x-radiographic technique allows us to not only observe the qualitative dynamic evolution of the shock wave but also derive thermodynamic parameters of interest. So, for example, the line-of-sight absorption data were used in a simple model-dependent approach to successfully deconvolute the mass density distribution and, subsequently, the pressure of SF_6 inside the shock front. Although radiography has long been used to image shock fronts in laser-solid interactions [16], to our knowledge, this is first time that x-radiography has been applied to directly image and quantify the thermodynamic parameters of shock waves generated by liquid jets in gaseous media.

Discussion

The dynamics of fuel injection in internal combustion engines provide an excellent example of why better experimental methods are needed for studying high-speed liquid jets. There has been relatively little progress in understanding fundamental processes in the so-called two-phase or multiphase fluid dynamics of high-speed jets that are central to every fuel injector. In the absence of such understanding, simultaneous optimization of the many variables associated with fuel injectors (e.g., nozzle shape and finish, fuel pressure, gas pressure, duration of injection) has been a highly empirical process, which effectively has amounted to educated wandering in a complex multidimensional space. Part of the reason for

the lack of progress has been the dearth of experimental methods to validate computational fluid dynamics modeling efforts. The x-radiographic method described here may well provide the needed information.

Acknowledgments

References

[1] J. D. O'Keefe, W. W. Wrinkle, and C. N. Scully, Nature **213**, 23-25 (1967).

[2] *Recent Advances in Spray Combustion: Spray Atomization and Drop Burning Phenomena,* edited by K. Kuo (American Institute of Aeronautics and Astronautics, Reston, VA, 1996), vols. 1 and 2.

[3] A. J. Yule and A. P. Watkins, Atomization and Sprays **1**, 441-465 (1991).

[4] N. Chigier, Prog. Energy Combust. Sci. **17**, 211-262 (1991).

[5] R. J. Adrian, Ann. Rev. Fluid Mech. **23**, 261-304 (1991).

[6] W. Hentschel and K.-P. Schindler, Opt. Laser Eng. **25**, 401-413 (1996).

[7] Z.-M. Cao, K. Nishino, S. Mizuno, and K. Torii, JSME Int. J. B-Fluid T. **43**, 582-589 (2000).

[8] Y.-Y. Zhang, T. Yoshizaki, and K. Nishida, Appl. Optics **39**, 6221-6229 (2000).

[9] C. F. Powell, Y. Yue, R. Poola, and J. Wang, J. Synchrotron Rad. **7**, 356-360 (2000).

[10] Y. Yue, C. F. Powell, R. Poola, J. Wang, and J. K. Schaller, Atomization and Sprays **11**, 471-490 (2001).

[11] A. MacPhee et al., Science **295**, 1261-1263 (2002).

[12] S. L. Barna et al., IEEE Trans. Nucl. Sci. **44**, 950-956 (1997).

[13] G. Rossi et al., J. Synchrotron Rad. **6**, 1096-1105 (1999).

[14] E. Hecht, *Optics,* 3rd ed. (Addison-Wesley, Reading, MA, 1998).

[15] J. J. Hurly, D. R. Defibaugh, and M. R. Moldover, Int. J. Thermophys. **21**, 739-765 (2000).

[16] D. Hoarty, A. Iwase, A. C. Meyer, J. Edwards, O. Willi, Phys. Rev. Lett. **78**, 3322-3325 (1997).